fibers

MDPI

Article

Optimising the Workability and Strength of Concrete Modified with Anacardium Occidentale Nutshell Ash

Solomon Oyebisi [1,*], Anthony Ede [1], Hilary Owamah [2], Tobit Igba [3], Oluwaseun Mark [1] and Abimbola Odetoyan [1]

[1] Department of Civil Engineering, Covenant University, PMB 1023 Ota, Nigeria; anthony.ede@covenantuniversity.edu.ng (A.E.); oluwaseun.mark@covenantuniversity.edu.ng (O.M.); abimbola.odetoyan@covenantuniversity.edu.ng (A.O.)
[2] Department of Civil and Environmental Engineering, Delta State University, Oleh Campus, PMB 1 Abraka, Nigeria; hiowamah@delsu.edu.ng
[3] Department of Civil Engineering, Federal University of Agriculture, PMB 2240 Abeokuta, Nigeria; igbaut@funaab.edu.ng
* Correspondence: solomon.oyebisi@covenantuniversity.edu.ng; Tel.: +234-7030-110-003

Abstract: Strength failure persists both in structural and mechanical analysis. One of its prominent characteristics is the adequate provision for parameters that minimise or maximise strength objectives while satisfying boundary conditions. The previous optimisation of concrete strength usually neglects mix design mechanisms induced by optimisation. Recent efforts to accurately optimise the concrete compressive strength have factored in some of these mechanisms. However, optimising concrete strength modified with high silica and alumina precursors, and crucial mix design factors are rare. Consequently, this paper optimised the concrete workability and strength, incorporating binding, water/binder ratio, binder/aggregate ratio, and curing mechanisms using the Box–Behnken design approach (BBDA). A waste material, anacardium occidentale (cashew) nutshell ash, was valorised and used at 5, 10, and 15 wt.% of cement. The composites were made, cured and tested at 14–90 d. The results revealed a high precision between the experimental slump and the optimisation slump at 97% R^2. In addition, a 5% increase in compressive strength was obtained compared with the target compressive strength. Besides, the correlation between the model equation obtained from this study and predictions of previous studies via BBDA yielded a strong relationship.

Keywords: cement; natural pozzolan; composite materials; compressive strength; workability; optimisation; response surface; modelling

Citation: Oyebisi, S.; Ede, A.; Owamah, H.; Igba, T.; Mark, O.; Odetoyan, A. Optimising the Workability and Strength of Concrete Modified with Anacardium Occidentale Nutshell Ash. *Fibers* **2021**, *9*, 41. https://doi.org/10.3390/fib9070041

Academic Editor: Giovanni Minafo

Received: 26 February 2021
Accepted: 26 April 2021
Published: 1 July 2021

1. Introduction

In recent times, the reality of material science as a subject area is still of interest considering the behavioural mechanisms of materials and the suitable modelling of their mathematical relationships [1]. A concrete mix is optimised to reduce the constituents' costs and expended time on conducting the concrete trial mixes without compromising the quality and performance of concrete under an applied loading condition [2]. Aggregates and cement paste are the primary constituents of concrete (composite material). Although the water/cement ratio governs the quality of required cement paste while the required proportion of cement paste to attain a targeted concrete strength and quality depends on the aggregates' characteristics such as types, voids, shapes, and surface area [2]. Therefore, as reported in previous studies [3–5], optimising a concrete mix can be conducted by adjusting the critical levels of mix factors such as binder/aggregate ratio, water/binder ratio, cementitious (binding) material contents, and binding contents ratio.

Box–Behnken design (BBD) is a statistical and analytical method of response surface that examines the effect of a set of quantitative experimental variables of factors on the response [6]. Response surface methodology (RSM), a design of experiment (DOE), is usually engaged to identify a set of vital factors (operating conditions), which generate the

"best" response [6,7]. Besides, RSM models a relationship between the quantitative factors and the response. Furthermore, BBD is a response surface three-level design where design points are either at the centre of the design or centred on the cube's edges, equidistant from the centre [6]. Unlike the central composite design of RSM, BBD allows efficient estimation of quadratic terms in a regression model and consists of fewer design points, hence less expensive to run [8]. Besides, BBD ensures that all design points fall within the safe operating limits (within the nominal high and low levels) for the process [6].

The early age compressive strength of concrete was conducted using RSM. The results indicated that the initial age strength could be predicted accurately via the developed models, which yielded about 85–90% coefficient of efficiency at 95% confidence bounds [9]. Dai et al. [10] optimised the mix quantities for cement paste backfill materials via RSM (four-factor and three-level). It was reported that the industrial standard backfilling materials was feasible and could be predicted via the RSM. Bahri et al. [11] also optimised the mix proportions of high strength-performance concrete modified with rice husk ash (RHA) using RSM (five-factor and three-level). The statistical findings revealed that the response models accurately optimised the responses, compressive strength and slump, at about 5% less error and significantly fit to predict the mix factors. Moreover, in an attempt to optimise the alkali-slag concrete (ASC) under freeze-thaw cycles, Liu et al. [12] adopted BBD. The results indicated that solutions ratio, slag content, and curing age (independent variables) were fitted accurately. The response models can be used to produce fracture toughness of alkali-slag concrete. A concrete modified with limestone filler was also optimised via RSM [13]. The statistical response models indicated an optimum validity for mixtures comprising water/limestone filler ratios of 0.38–0.72 at 120 kg/m^3 of limestone filler and 250–400 kg/m^3 of cement. Despite the previous studies on optimising concrete mixtures incorporating supplementary cementitious materials (SCMs), no research is available to optimise a concrete mix modifying with cashew nut shell ash (CNA).

The utilisation of SCMs in concrete production reduces the constituents' costs, energy consumption, and environmental impacts, contributing to energy and environmental preservation and sustainable products and development [14]. Oyebisi et al. [15] investigated the reactivity indexes and durability properties of geopolymer concrete (GPC), incorporating both ground granulated blast furnace slag (GGBFS) and corn cob ash (CCA) as SCMs. The results indicated that GGBFS and CCA's oxide compositions enhanced the reactivity, compressive strength, and chemical resistance of GPC produced. Moreover, Mark et al. [16] reviewed the effects of some SCMs, cupola furnace slag powder (CFSP), blast furnace slag powder (BFSP), silica fume (SF), fly ash (FA), rice husk ash (RHA), metakaolin (MK), coconut husk ash (CHA), palm oil fuel ash (POFA), wood waste ash (WWA), sugar cane bagasse ash (SCBA), corn cob ash (CCA), and bamboo leaf ash (BLA), on the workability and compressive strength of concrete. It was revealed that the incorporation of these twelve SCMs significantly improved the strength and workability of concrete. Akinwumi and Aidomojie [17] examined the influence of corncob ash on lateritic soil's geotechnical properties stabilised with Portland cement. The results showed that incorporating CCA into the soil generally reduced its plasticity, swell potential, and permeability. It also increased the soil's strength. Besides its economic and environment-friendly characteristics compared with the cement-stabilisation, CCA improved the soil's geotechnical properties for pavement layer material application. At 25–50% of SCMs by wt.% of cement, there are about 20–67% and 33–80% reduction in required energy and material cost, respectively [18]. Consequent to the broader utilisation of some SCMs, CNA's use as SCM in concrete production is rare. Cashew nutshell is a waste product obtained from agricultural produce. In 2017, about 4.5 million metric tonnes (MMT) was generated globally, with Nigeria generating about 0.1 MMT [19]. From 2.5 MMT of cashew nuts generation, about 1.825 MMT of waste is obtained [20]. However, it is worrisome to observe that this material is usually discarded as waste, causing environmental problems.

In this present study, an attempt was made to engage the application of a BBD of RSM to obtain an optimum proportioning of concrete strength using the values obtained from an

experimental design. Design factors such as binders' ratio, water/binder ratio, curing ages, and binder/aggregate ratio were selected as independent (continuous) variables. At the same time, the compressive strength was considered as a response variable. The data were analysed statistically via Minitab 17 software, and the regression model was developed for concrete strength as a function of mixture variables. The developed approach to optimising the mixtures of concrete proportions was based on the experimental works (involving the required characteristics of concrete performance) and the statistical analysis of data generated; this would reduce time, cost, and the number of trial mixes.

2. Materials and Methods

2.1. Materials' Preparation and Characterisations

Cashew nutshell was valorised using the pyrolysis method, and about 23 wt.% of cashew nutshells was obtained as ash. The results of chemical compositions of the ash and Portland limestone cement (PLC) used, via XRF analyser, Model PW-1800, are presented in Table 1. The results indicated that cashew nutshell ash (CNA) met a 70% minimum required specification of SiO_2 + Al_2O_3 + Fe_2O_3, recommended by BS EN 8615-2 [21], hence suitable for use as SCM. A 42.5 R PLC was used as a binder. Moreover, the fineness, specific gravity, and specific surface area were obtained for both CNA and PLC as 8.10 and 3.15%, 2.85 and 3.15 g/cm^3, and 505 and 375 m^2/kg, respectively, following the procedure outlined in BS EN 196-3 [22]. The particle size distribution (PSD) of the binders, as shown in Figure 1, was evaluated using Laser diffraction, Model Beckman Coulter LS-100. The results signified that more volume and water would be needed, and a higher capacity against an alkaline environment would be yielded when CNA replaces PLC [23].

Table 1. Oxide compositions of the binding materials used.

Oxide Composition	CaO (%)	SiO_2 (%)	Al_2O_3 (%)	Fe_2O_3 (%)	MgO (%)	K_2O (%)	Na_2O (%)	SO_3 (%)	TiO_2 (%)	P_2O_5 (%)	LOI (%)
AONSA	2.04	65.02	16.28	10.16	1.53	0.52	0.45	1.32	0.01	0.01	2.95
PLC	65.5	21.55	5.5	3.08	1.52	0.61	-	2.03	-	-	1.2

LOI = loss of ignition, determined at 800 °C.

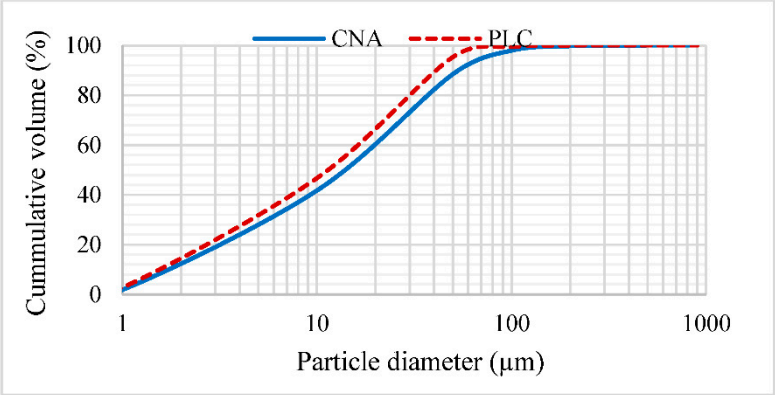

Figure 1. The PSD of binding materials used.

Aggregates, fine aggregate (≤4.5 mm size) and coarse aggregate (granite 12.5 mm size) were used. The specific gravity (SG) and water absorption (WA) of aggregates were determined by weighing 2 kg of each sample, immersing in clean water at 25 °C for 24 h and drying in an oven for 24 h at 110 °C [11]. The WA results indicated 0.70 and 0.80% and 2.60 and 2.65 g/cm^3 for both fine aggregates (FA) and coarse aggregates (CA). In addition the moisture content (MC) was examined using a clean container covered with a lid. A 2 kg of each sample was oven-dried at 105 °C for 24 h, removed and cooled for 45 min, and then weighed. The results showed 0.3% and 0.2% MC for both FA and CA, respectively.

As outlined in BS EN 12620 [24], Grading was conducted on the aggregates used, and the results are shown in Figure 2.

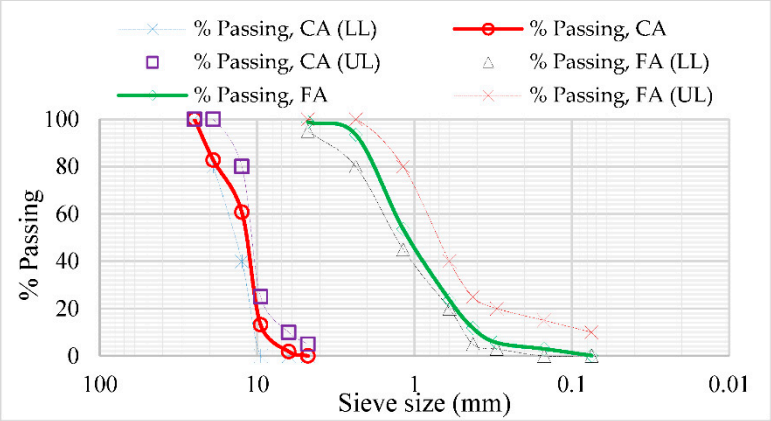

Figure 2. The PSD of aggregates used. CA is coarse aggregate, FA is fine aggregate, and LL and UL are lower and upper limits.

2.2. Design Proportions and Concrete Strength Specifications

BS EN 206 [25] was used to design the trial mix proportions, considering the materials' physical characteristics. Portland limestone cement (PLC) was replaced with CNA at 5, 10, and 15 wt.% proportions because a 15% maximum substitution of PLC with CNA exhibited an optimum compressive strength for structural applications [26,27]. Concrete grades M 25, M 30, and M 40 targeted the respective concrete strengths 25, 30, and 40 MPa at 28 days curing were adopted due to their general uses in the building construction. Ultimately, the trial mix design results are presented in Tables 2–4 for M 25, M 30, and M 40, respectively.

Table 2. Mix design proportions for M 25.

Mix ID	PLC (kg/m^3)	CNA (kg/m^3)	FA (kg/m^3)	CA (kg/m^3)	Water/Binder Ratio	Binder/Aggregate Ratio
V0	340	0	715	1035	0.62	0.19
V1	323	17	715	1035	0.62	0.19
V2	306	34	715	1035	0.62	0.19
V3	289	51	715	1035	0.62	0.19

Table 3. Mix design proportions for M 30.

Mix ID	PLC (kg/m^3)	CAN (kg/m^3)	FA (kg/m^3)	CA (kg/m^3)	Water/Binder Ratio	Binder/Aggregate Ratio
X0	390	0	675	1031	0.52	0.25
X1	370	20	675	1031	0.52	0.25
X2	350	40	675	1031	0.52	0.25
X3	330	60	675	1031	0.52	0.25

Table 4. Mix design proportions for M 40.

Mix ID	PLC (kg/m^3)	CAN (kg/m^3)	FA (kg/m^3)	CA (kg/m^3)	Water/Binder Ratio	Binder/Aggregate Ratio
Z0	500	0	585	1030	0.42	0.31
Z1	475	25	585	1030	0.42	0.31
Z2	450	50	585	1030	0.42	0.31
Z3	425	75	585	1030	0.42	0.31

2.3. Sample Preparations and Experimental Tests

The mixing was carried out for about 15 min at 25 ± 3 °C temperature and 65 ± 5% relative humidity. The slump and density tests were performed on the concrete specimens outlined in BS EN 12350-2 [28] and BS EN 12390-7 [29], respectively. The slump cone mould was filled with fresh concrete in three equal layers and compacted with 35 tamping rod strokes. The mould was vertically lifted upward, and then the height difference between the collapsed concrete and the slump cone was measured. For the compressive strengths, mixes were prepared using the standard cube 150 mm^3 and crushed at 14–90 d following the BS EN 12390-3 [30]'s procedure. The cubes were removed from the moulds after 24 h and immersed in a curing tank for 14–90 d at 25 ± 3 °C temperatures and 65 ± 5% relative humidity. The force was applied to the concrete cube in a constant regime under a loading rate of 0.6 MPa per second until failure occurs. The values at failure were taken, and the mean of 3 crushed samples was used for the statistical analysis.

2.4. Box-Behnken Design (BBD)

The BBD was applied to evaluate the interaction between the selected continuous variables and the response variable. Minitab statistical software was used, and the BBD was created using the four (4) different continuous variables, as shown in Table 5. Thus, the experimental run number was estimated using the illustration presented in Equation (1) [6]. However, the optimisation of workability (slump) was statistically evaluated using the selected continuous variables, as shown in Table 5, except curing age (D), because slump is determined immediately after the mixing process, requiring no curing period.

$$N = 2v(v-1) + c_p \quad (1)$$

where N is the number of experimental runs, v is the total continuous variables, and c_p is the total applied central point.

Table 5. Four continuous variables in a three different levels for BBD.

Variables	Symbol	Coded Values		
		Low	Centre	High
		−1	0	+1
Water/binder	A	0.42	0.52	0.62
Binder/aggregate	B	0.19	0.25	0.31
CNA/(CNA + PLC)	C	0.05	0.10	0.15
Curing age	D	14	52	90

Following Equation (1), the number of the experimental run based on four (4) continuous variables and three (3) applied central points, as shown in Table 5, was twenty-seven (27). Besides, the full quadratic term, as illustrated in Equation (2), accurately optimises the relationship between the continuous variables and the response variable, hence yielding a high precision [6,8].

$$Y = a_0 + \sum_{i=1}^{n} a_i x_i + \sum_{i=1}^{n} a_{ii} x_i^2 + \sum_{i<j} a_{ij} x_i x_j \quad (2)$$

where Y is the response variable (f_c), a_0 is model coefficient constant, x_i and x_j are continuous variables, a_i is the linear coefficient, a_{ii}: square coefficient, and a_{ij} is the interaction coefficient.

2.5. Optimisation of Variables

The four continuous variables were minimised while maximising the response variable (compressive strength) via the optimisation concept. Based on this concept, the response variable was converted into a composite desirability function (*CD*) over the range of 0–1,

as illustrated in Equation (3) [6,7]. Consequently, the closer the composite desirability to 1, the better the optimisation [6,7].

$$0 \leq CD \leq 1 \tag{3}$$

From Equation (3), $CD = 1$ if the response value (compressive strength) is at its goal or target. Besides, $CD = 0$ if the response value is outside an acceptable region. The desirability is a composite based on the expressions illustrated in Equations (4)–(6) to maximise, minimise, and to make the response to be as close as possible to the target, respectively [6]. Therefore, Equations (4)–(6) were used to validate the optimisation study results.

$$\begin{cases} D = 0 \text{ if } r \leq L \\ CD = \left(r - \frac{L}{T} - L\right)^{w} \text{ if } L \leq r \leq T \\ D = 1 \text{ if } r \geq T \end{cases} \tag{4}$$

$$\begin{cases} D = 1 \text{ if } r \leq T \\ CD = \left(r - \frac{U}{T} - U\right)^{w} \text{ if } T \leq r \leq U \\ D = 0 \text{ if } r \geq U \end{cases} \tag{5}$$

$$\begin{cases} CD = \left(r - \frac{L}{T} - L\right)^{w1} \text{ if } L \leq r \leq T \\ D = 1 \text{ if } r = T \\ CD = \left(r - \frac{U}{T} - U\right)^{w2} \text{ if } T \leq r \leq U \\ D = 0 \text{ if } r = L \\ D = 0 \text{ if } r = U \end{cases} \tag{6}$$

where CD is the composite desirability function (0–1), r is the response, L, U, and T are lower, upper, and target values/limits, respectively, and w is the weight.

2.6. Statistical Analysis and Fitting of the Strength Model

In analysing the experimental data, analysis of variance (ANOVA) was used to evaluate the four continuous variables, as presented in Table 5 and considered for the development of compressive strength and the statistical model's fitting using the full quadratic terms. Degree of freedom (DF) is one of the statistical terms in ANOVA, which defines the number of final values (n) in the statistical analysis that is freely bound to change. The relationship is presented in Equation (7).

$$DF = n - 1 \tag{7}$$

An adjusted sum of square ($Adj\ SS$) is the adjusted squared distance, as illustrated in Equation (8) for summation of all data points (n), between each observed data (Y) and the sample mean (Z) [2]. Moreover, the adjusted mean square ($Adj\ MS$), as illustrated in Equation (9), represents $Adj\ SS$ ratio to the DF.

$$Adj\ SS = \sum_{i=1}^{n} (Y - Z)^2 \tag{8}$$

$$Adj\ MS = \frac{Adj\ SS}{DF} \tag{9}$$

F-value signifies a ratio of $Adj\ MS$ of the continuous factor to the $Adj\ MS$ of the error. In the statistical analysis, an error (residual) connotes the statistical difference between the observed variables and the adopted model's predicted values. Thus, a factor with a significant effect yields a higher F-value [2]. P-value represents a significance level

compared with the α-value of 0.05. Considering the null hypothesis, if *P*-value ≤ α-value, there is a significant effect; if *P*-value > α-value, then no significant impact [2].

3. Results and Discussion

3.1. Slump, Density, and Compressive Strengths

The slump results for M 25–40 are presented in Figure 3. The results indicated that the slump decreased as CNA content increased. About 13–33%, 14–36%, and 8–33% decrease in slump were observed for concrete grades M 25, M 30, and M 40, respectively, as the CNA content increased from 5–15%. The reason could be associated with CNA's physical characteristics, finer particle size, and lower SG compared with PLC. Consequently, water demand increased owing to more volume as CNA replaced PLC; this resulted in more cohesive concrete, hence reducing the concrete's workability [23]. The incorporation of finer pozzolans (cashew nutshell and rice husk ashes), as reported in previous studies, reduced the concrete slump in its fresh state [26,31]. Thus, a concrete modifying with CNA could be a workable mix of 15% substitution because an optimum slump of 150 mm for normal workable concrete specified by BS EN 12350-2 [28] was satisfied.

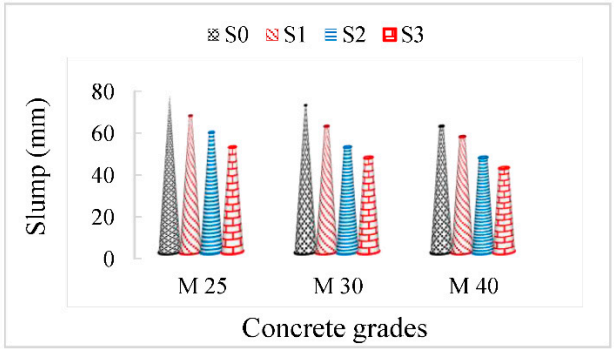

Figure 3. The slump results. S0 (100% PLC), S1 (95% PLC + 5% CNA), S2 (90% PLC + 10% CNA), S3 (85% PLC + 15% CNA).

Figure 4 indicates the results of the density test at 28 days curing. From Figure 4, the density decreased with increasing CNA content. Comparing with the control sample (S0), there was about 3–10% decrease in density as wt.% of CNA increased from 5–15% for all concrete grades. The decline in density with increasing CNA content could be attributed to the SG of CNA, which was 10% lesser than that of PLC; this reduced the interfacial particle of PLC, hence decreasing the density. These results also supported the findings from previous studies [32,33], which reported that an increase in pozzolan content (CNA in this case) in the cement-pozzolan based concrete reduces the density of the tiny air bubbles of the pozzolan in the cementitious matrix. It was also evident from Figure 4 that the density increased as the concrete grades increased from M 25–M 40 due to denser, less porous, and low water content of the concrete mix [23]. Therefore, the partial substitution of PLC by CNA reduces the dead loads, contributing to the lightweight of a building.

As shown in Figure 5a–c, the concrete's compressive strengths (fc) increased with increasing CNA content. As the percentage substitution of CNA content increased from 5–15%, there was about 3–6% increase in strength for M 25–M 40 at 28 d curing than the control sample (100% PLC). The reason for strength increment could be attributed to the substantial contents of SiO_2 and Al_2O_3 of CNA compared with PLC, which reacted with the cement's hydrating agents and resulted in the C-S-H and C-A-H; these are concrete's strengthening gel and bond, respectively [23]. Therefore, CNA could be used at 5–15% replacement level for structural applications because all concrete grades fulfilled the target strengths specified by BS EN 1992-1-1 [34] at 28 d curing.

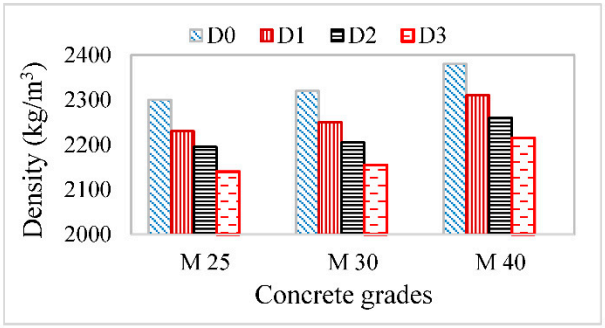

Figure 4. The density of concrete grades. D0 (100% PLC), D1 (95% PLC + 5% CNA), D2 (90% PLC + 10% CNA), D3 (85% PLC + 15% CNA).

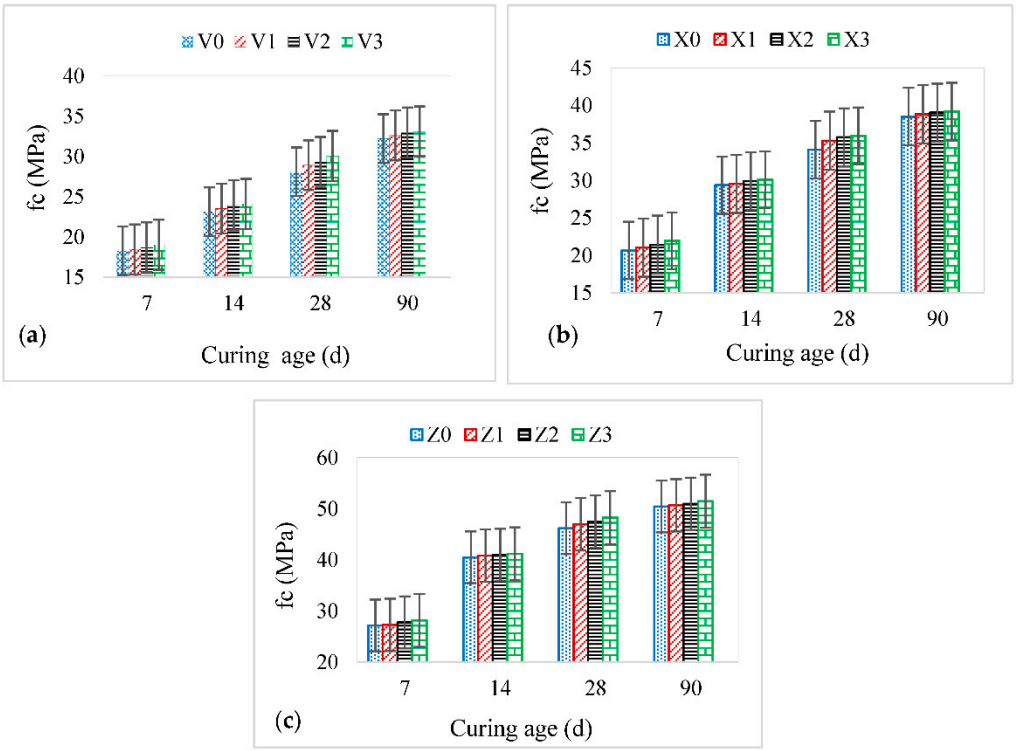

Figure 5. The results of compressive strengths for concrete grades (**a**) M 25, (**b**) M 30, and (**c**) M 40.

3.2. Design of Experiment (DOE)

Following the creation of response surface design in Minitab 17 using BBD with four continuous variables, as presented in Table 5, the statistical results are presented in Table 6. The fitted model analysis results to a response surface design are presented in Table 7. The linearly squared terms yielded the best precision and significant effect compared to the full quadratic terms, hence used for the modelling analysis. However, in modelling, both A^2 and B^2 were adjudged as nonsignificant terms and removed from the model. ANOVA examined the model's accuracy on continuous variables' influence on the compressive strength (fc).

As revealed in Table 7, all terms, except A and C^2, exhibited significant concrete strength effects because *P*-value was less than α-value (0.05). Consequently, the regression model between the response variable (fc) and the continuous variables (A, B, C, and D) is developed, as illustrated in Equation (10), for the concrete grades, water/binder ratio, binder/aggregate ratio, CNA/(CNA + PLC), and curing ages ranging from M 25–M 40, 0.42–0.62, 0.19–0.31, 0.05–0.15, and 14–90 d, respectively. Moreover, the model's goodness of

fits yielded standard distance (S) and coefficient of determination (R^2) as 0.279352 and 100%, respectively; this signified that the model is 100% fit to optimise all designed variables.

$$f_c = 1.61 - 16.11A + 121.7B - 9.37\,C + 0.6379D - 10.0C^2 - 0.004938D^2 \quad (10)$$

Table 6. Results of the response surface design using BBD.

Run Order	Block	A	B	C	D	fc (MPa)
1	1	0.52	0.25	0.15	28	35.95
2	1	0.52	0.25	0.10	14	29.92
3	1	0.42	0.31	0.05	28	46.94
4	1	0.52	0.25	0.15	90	39.21
5	1	0.62	0.19	0.05	28	28.94
6	1	0.42	0.31	0.15	28	48.25
7	1	0.62	0.19	0.15	28	30.07
8	1	0.62	0.19	0.10	90	32.97
9	1	0.62	0.19	0.10	14	23.95
10	1	0.52	0.25	0.05	28	35.29
11	1	0.52	0.25	0.05	14	29.55
12	1	0.42	0.31	0.10	14	40.97
13	1	0.52	0.25	0.10	90	39.05
14	1	0.52	0.25	0.05	90	38.83
15	1	0.62	0.19	0.15	90	33.10
16	1	0.52	0.25	0.15	14	30.11
17	1	0.42	0.31	0.05	90	50.65
18	1	0.62	0.19	0.10	28	29.32
19	1	0.42	0.31	0.10	90	50.93
20	1	0.42	0.31	0.10	28	47.49
21	1	0.62	0.19	0.15	14	24.11
22	1	0.62	0.19	0.05	14	23.15
23	1	0.52	0.25	0.10	28	35.75
24	1	0.42	0.31	0.15	90	51.48
25	1	0.42	0.31	0.05	14	40.83
26	1	0.42	0.31	0.15	14	41.16
27	1	0.62	0.19	0.05	90	32.63

A is water/binder ratio, B is binder/aggregate ratio, C is CNA/(CNA + PLC), and D is curing age (d).

Table 7. ANOVA for the regression model using linearly squared terms.

Source	*DF*	*Adj SS*	*Adj MS*	*F*-Value	*P*-Value
Model	11	1890.93	315.154	4038.49	0.000
Linear	4	1880.78	470.196	6025.23	0.000
A	1	0.27	0.267	3.42	0.079
B	1	5.61	5.615	71.95	0.000
C	1	2.44	2.442	31.29	0.000
D	1	402.33	402.334	5155.63	0.000
Square	2	97.29	48.643	623.32	0.000
C^2	1	0.00	0.004	0.05	0.829
D^2	1	97.28	97.282	1475.79	0.000
Error	20	1.56	0.078	-	-
Total	26	1892.49	-	-	-

A is water/binder ratio, B is binder/aggregate ratio, C is CNA/(CNA + PLC), and D is curing age (d).

In practice, a balanced or nearly balanced design with a large number of observations does not significantly influence the residuals (the difference between the observed and the fitted response variable) if it departs moderately from a straight line or normality [6]. Thus, normally distributed residuals from the analysis are required for a balanced design. As shown in Figure 6, the residuals generally followed a straight-line pattern, hence no evidence of non-normality or unknown variables in the model. Furthermore, in a designed experiment, the order of observations influences the response

variable if the residuals fluctuate in a random pattern around the centre line [6]. The result of versus order for the response variable, as shown in Figure 7, exhibited a randomly scattered pattern about zero, hence indicating that no evidence exists that the error terms are correlated with one another.

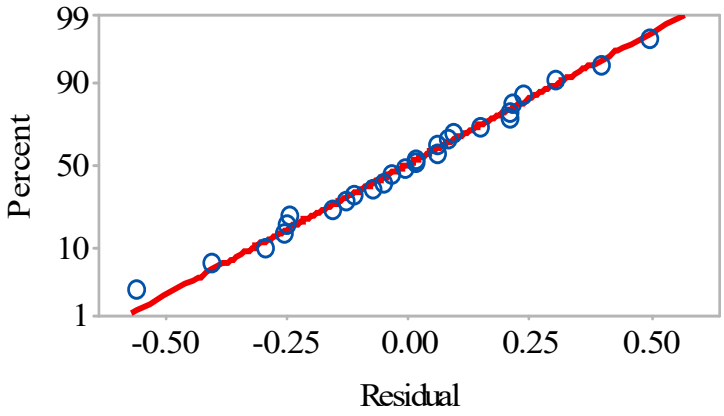

Figure 6. The normal probability plot for the response (fc).

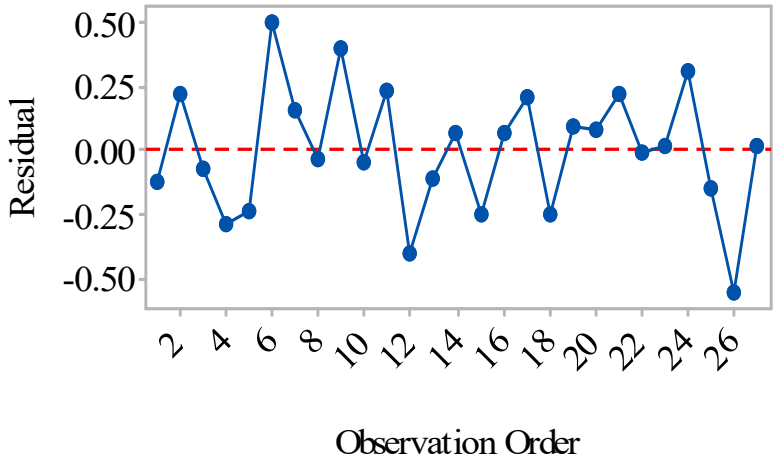

Figure 7. Residual versus observation order plot.

In optimising the workability (slump), linear term exhibited the best and significant effects compared with linearly squared, linearly interacted, and full quadratic terms. However, during the statistical analysis, the binder/aggregate ratio (B) could not be estimated and was removed. The binder/aggregate ratio (B) could not contribute to the response because it was statistically insignificant [8]. Moreover, concrete's slump is majorly influenced by binders' physical characteristics and the water/binder ratio [23]. Thus, the model summary is illustrated in Equation (11), yielding R^2 as 97%. This signifies that the model can optimise and predict the slump (S) of fresh concrete incorporating CNA for all designed factors at 95% confidence and prediction bounds for the concrete grades, water/binder ratio (A), binder/aggregate ratio (B), and CNA/(CNA + PLC) (C) ranging from M 25–M 40, 0.42–0.62, 0.19–0.31, and 0.05–0.15, respectively. Figure 8 presents the relationship between the optimisation slump (OS) and the experimental slump (ES).

$$S = 35.89 + 60\mathrm{A} - 149.25\mathrm{C} \quad (11)$$

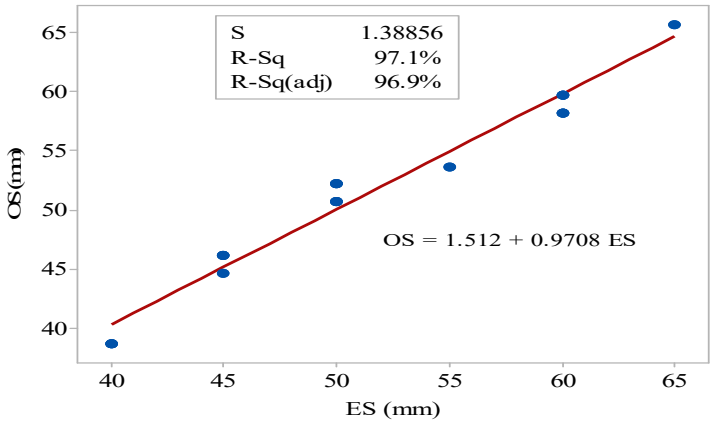

Figure 8. Correlation between optimisation slump (OS) and experimental slump (ES).

3.3. Main Effects of Continuous Variables on fc

The main effects of continuous variables on the response variable (fc) are presented in Figure 9 following the fitted model generation based on the stored model. It was evident from Figure 8 that the continuous variables influenced the response variable because the plotted lines were not horizontal [6]. An increase in curing age (D), binder/aggregate ratio (B), cementitious content (C), as shown in Figure 9, improved the concrete strength (fc). However, the main effects of curing age on the response (fc) signified that the strength could be optimised at 65 d against 90 d, hence minimising the curing time by about 28%. This result supported the findings of similar study [5] where the compressive strengths of geopolymer concrete incorporating corncob ash as SCM were optimised at 74 d and 83 d curing for concrete grades M 30 and M 40, respectively. Moreover, the concrete strength increased at a low water/binder ratio (A) compared with a high water/binder ratio due to the hydration process rate. The low water/binder content accelerates the setting times, compacts the matrix mechanism, and minimises the matrix pores, resulting in higher strength performance [32]. As reported in the previous studies [32,35], it was confirmed that higher cementitious and binder/aggregate contents with low water/binder ratio result in a higher compressive strength due to mechanical interlocking and cracking-arresting capacities of the cement-aggregate bond.

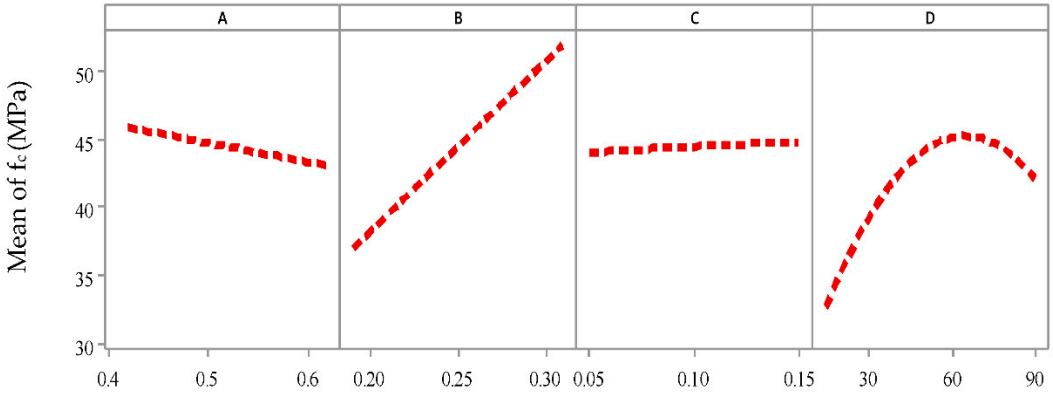

Figure 9. The main effect of continuous variables on response value. A is water/binder ratio, B is binder/aggregate ratio, C is CNA/(CNA+PLC), and D is curing age (d).

3.4. Operating Conditions of Continuous Variables on fc

Operating conditions illustrate the interaction between the continuous variables and the response variable and visualise the effects in both 2-D contour lines and 3-D surface, holding other continuous variables constant. The contour indicates the highest impact on

the operating condition with the darkest green colour. Notwithstanding, any alteration to the continuous variables would change the shape patterns of the working conditions.

3.4.1. Influence of A and B on fc

Figure 10a,b present the visualised effects on fc in 2-D contour lines and 3-D surface, respectively. As shown in Figure 10, it was evident that the strength increased with increasing B but at a decreasing A, holding both C and D at 10% and 52 d constant, respectively. Therefore, a response (fc) greater than 52 MPa, could be attained at 0.31 and 0.42 for B and A, respectively.

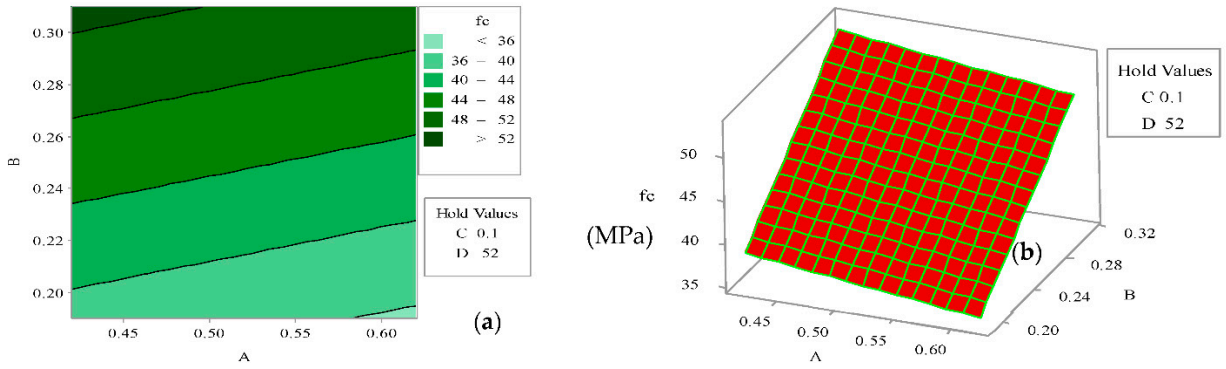

Figure 10. Effects of B and A on fc (MPa) (**a**) 2-D contour lines (**b**) 3-D surface. A is water/binder ratio, B is binder/aggregate ratio, C is CNA/(CNA + PLC), and D is curing age (d).

3.4.2. Influence of D and A on fc

The visualised effects of D and A on fc are presented in Figure 11a,b for 2-D contour lines and 3-D surface, respectively. It was revealed that the response (fc) could be optimised (˃45 MPa) at about 65 d of curing age (D) and a low water/binder ratio $\leq$ 0.42, holding both B and C at 0.25 and 10% constant, respectively.

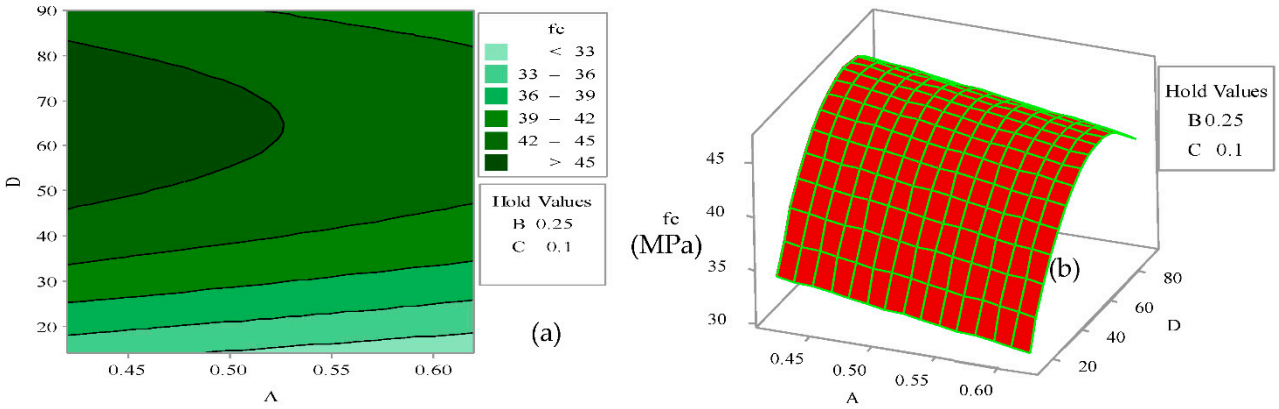

Figure 11. Effects of D and A on fc (MPa) (**a**) 2-D contour lines (**b**) 3-D surface. A is water/binder ratio, B is binder/aggregate ratio, C is CNA/(CNA + PLC), and D is curing age (d).

3.4.3. Influence of D and B on fc

As shown in Figure 12a,b, the response (fc) increased with increasing D and B, holding A and C at 0.52 and 10%, respectively. However, the interaction revealed that the response could be optimised (˃50 MPa) at about 65 d of curing age and 0.31 B.

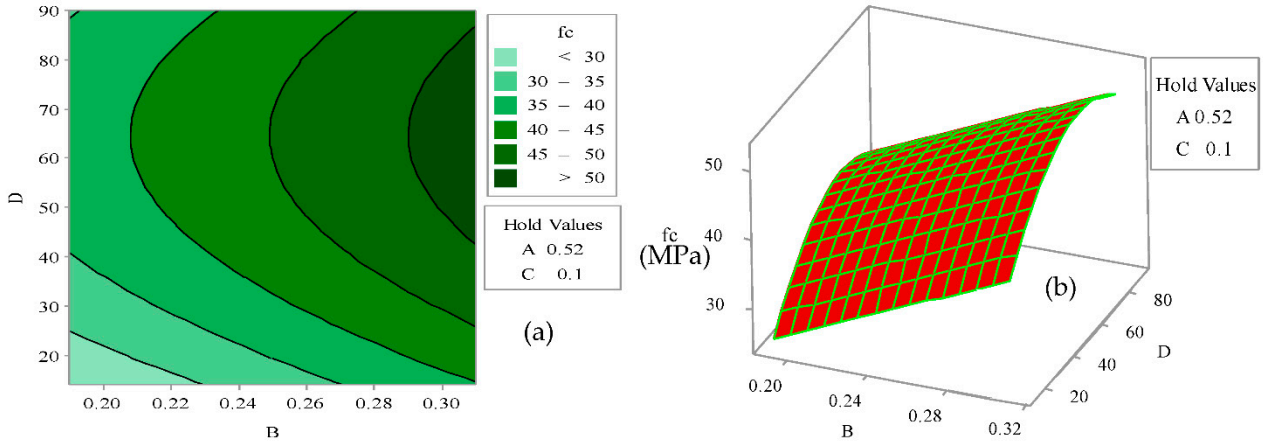

Figure 12. Effects of D and B on fc (MPa) (**a**) 2-D contour lines (**b**) 3-D surface. A is water/binder ratio, B is binder/aggregate ratio, C is CNA/(CNA + PLC), and D is curing age (d).

3.5. Optimisation

Based on the model stored, Figure 13 presents the optimisation results for the response (fc) following the desirability functions' combination into single composite desirability (CD). The vertical brown and horizontal blue lines, as shown in Figure 13, signified a current setting and a current response (fc), respectively. The current set showed A, B, C, and D as 0.42, 0.31, 0.15, and 70 d, respectively, yielding an optimised response (fc) of 54 MPa at 1.000 composite desirability (CD). Therefore, the strength optimisation results supported a relationship, as illustrated in Equation (10), such that CD = 1 because the current response, fc (54 MPa), is higher than the target/upper strength (51.48 MPa) obtained from the experimental works.

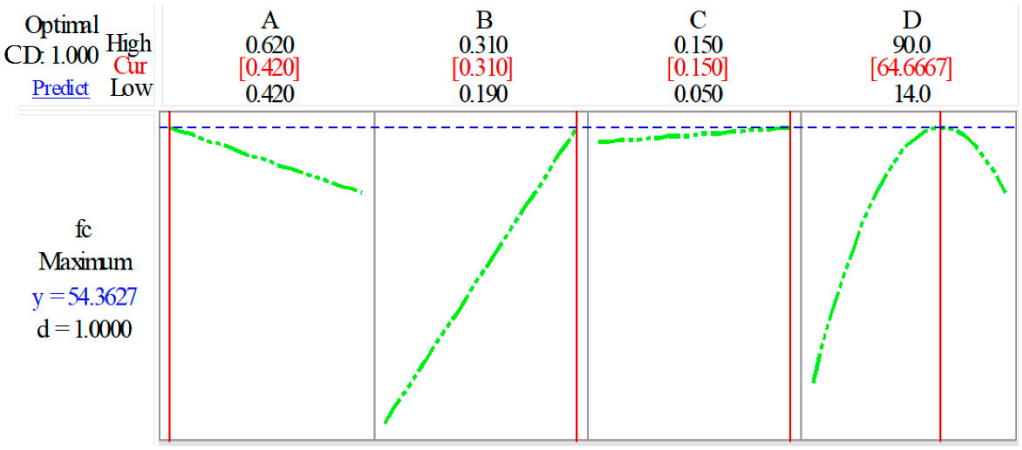

Figure 13. Optimisation plot for the response (fc, MPa). A is water/binder ratio, B is binder/aggregate ratio, C is CNA/(CNA+PLC), and D is curing age (d).

3.6. Comparison of Developed Model with the Previous Studies

Figure 14 compares the developed model with the earlier studies to establish and prove the model's accuracy, precision, and actual forecasting capability toward the concrete modifying with SCMs. As indicated in Figure 14, Kumar and Prasad [36] replaced fly ash and silica fume at 6–15 wt.% of cement using a design water/binder and binder/aggregate ratios of 0.4–0.5 and 0.21–0.22, respectively. Moreover, Duana et al. [37] substituted both metakaolin and blast furnace slag at 10–20 wt.% of cement using water/binder and binder/aggregate ratios of 0.50 and 0.20, respectively. Compared the experimental compressive strengths (Efc) of these previous studies [36,37] with the developed model, as illustrated in Equation (10), the predictive results (Pfc) yielded a high precision with

62–88% R^2, hence indicating a good relationship. Therefore, this developed model established the reliability to predict and optimise the concrete compressive strength, mainly modified and produced with SCMs.

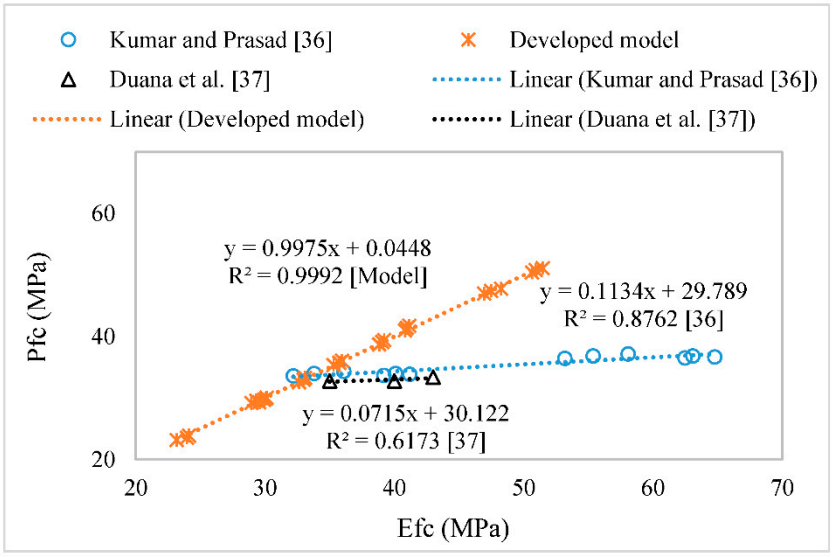

Figure 14. Comparison of the developed model with previous studies.

4. Conclusions

A simplified mechanism, optimising the concrete workability and strength modified with high silica and alumina precursor, was developed based on the statistical analysis obtained through an experimentally designed work. As a result of this mechanism, the following outcomes are drawn: At 5–15 wt.% substitution of CNA, there was about 3–6% increase in concrete's compressive strengths for all concrete grades (M 25, M 30, and M 40) at 28 d curing. Moreover, the optimum values of water/binder ratio (A), binder/aggregate ratio (B), and SCM/cement ratio (C) exhibited a 5% increase in compressive strength at 28% decrease in curing age (D) compared with the target variables. This signifies a significant cost and time saving while maintaining the composite product's quality and strength performance. On the other hand, as illustrated in Equation (10), the developed model has proved to be efficient such that a good relationship with high precision was obtained when compared with the previous concrete strength incorporating SCMs. In addition the slump obtained via optimisation and that of experimental values yielded the same results, hence exhibiting a strong precision, as illustrated in Equation (11); this can be used in the prediction of normal workability of concrete modified with CNA while saving cost and time of preparing experimental works. Finally, the possibility of using less water for the optimisation of concrete strength is attainable by blending PLC with anacardium occidentale nutshell ash (cashew nutshell ash, CNA). In addition this research can be applied in the normal reinforced concrete work without vibration.

Author Contributions: Conceptualisation, S.O.; data curation, S.O.; methodology, S.O.; validation, A.E., H.O. and A.O.; formal analysis, S.O.; investigation, S.O.; resources, S.O., A.E. and A.O.; writing—original draft preparation, S.O.; writing—review and editing, H.O., T.I. and A.O.; visualisation, S.O., T.I. and A.O.; supervision, S.O.; project administration, S.O., O.M., T.I. and H.O.; software, S.O.; funding acquisition, S.O., A.E., O.M. and A.O. All authors have read and agreed to the published version of the manuscript.

Funding: Funding for open access charge: Covenant University Centre for Research, Innovation and Discovery (CUCRID).

Institutional Review Board Statement: Not applicable.

Informed Consent Statement: Not applicable.

Data Availability Statement: The data presented in this study are available on request from the corresponding author.

Acknowledgments: The authors acknowledged the technical support from the Structural and Materials Laboratory of Civil Engineering Department, Covenant University.

Conflicts of Interest: The authors declare no conflict of interest.

References

1. Angelo, M.D.; Placidi, L.; Nejadsadeghi, N.; Misra, A. Non-standard Timoshenko beam model for chiral metamaterial: Identification of stiffness parameters. *Mech. Res. Commun.* **2020**, *103*, 103462. [CrossRef]
2. Ahmad, S.; Alghamdi, S.A. Statistical approach to optimising concrete mixture design. *Sci. World J.* **2014**, *561539*, 1–7.
3. Chang, P.K. An approach to optimising mix design for properties of high-performance concrete. *Cem. Concr. Res.* **2004**, *34*, 623–629. [CrossRef]
4. Ozlem, A.; Ulas, A.K.; Bahar, S. Self-consolidating high strength concrete optimisation by mixture design method. *ACI Mater. J.* **2010**, *107*, 357–364.
5. Oyebisi, S.O.; Ede, A.N.; Olutoge, F.A. Optimization of design parameters of slag-corncob ash-based geopolymer concrete by the central composite design of the response surface methodology. *Iran. J. Sci. Technol. Trans. Civ. Eng.* **2021**, *45*, 27–42. [CrossRef]
6. Myers, R.H.; Montgomery, D.C.; Anderson-Cook, C.M. *Response Surface Methodology: Process and Product Optimisation Using Designed of Experiments*, 3rd ed.; John Wiley and Sons, Inc.: Hoboken, NJ, USA, 2009.
7. Myers, R.C.; Montgomery, D.C.; Vining, G.G.; Borror, S.M.; Kowalski, S.M. Response surface methodology: A retrospective and literature survey. *J. Qual. Technol.* **2004**, *36*, 53–77. [CrossRef]
8. Montgomery, D.C. *Design and Analysis of Experiments*, 6th ed.; John Wiley and Sons, Inc.: Hoboken, NJ, USA, 2005.
9. Alsanusi, S.; Bentaher, L. Prediction of compressive strength of concrete from early age test result using design of experiments (RSM). *Int. J. Civ. Environ. Eng.* **2015**, *9*, 1559–1563.
10. Dai, C.; Wu, A.; Qi, Y.; Chen, Z. The optimisation of mix proportions for cement paste backfill materials via Box–Behnken experimental method. *J. Inst. Eng. India Ser. D* **2019**, *100*, 307–316. [CrossRef]
11. Bahri, S.; Mahmud, H.B.; Shafigh, P. Optimisation of mixture proportions of high strength high-performance concrete incorporating rice husk ash by using response surface methodology. In Proceedings of the 1st Workshop on the Multidisciplinary and Its Applications, Part 1, Aceh, WMA-01, Aceh, Indonesia, 19–20 January 2018.
12. Li, Q.; Cai, L.; Fu, Y.; Wang, H.; Zou, Y. Fracture properties and response surface methodology model of alkali-slag concrete under freeze-thaw cycles. *Constr. Build. Mater.* **2015**, *93*, 620–626. [CrossRef]
13. Ghezal, A.; Khayat, K.H. Optimising self-consolidating concrete with limestone filler by using statistical factorial design methods. *ACI Mater. J.* **2002**, *99*, 264–272.
14. Farinha, C.B.; Silvestre, J.D.; de Brito, J.; Veiga, M.R. Life cycle assessment of mortars with incorporation of industrial wastes. *Fibers* **2019**, *7*, 59. [CrossRef]
15. Oyebisi, S.; Ede, A.; Olutoge, F.; Ogbiye, S. Evaluation of reactivity indexes and durability properties of slag-based geopolymer concrete incorporating corn cob ash. *Constr. Build. Mater.* **2020**, *258*, 119604. [CrossRef]
16. Mark, O.G.; Ede, A.N.; Olofinnade, O.; Bamigboye, G.; Okeke, C.; Oyebisi, S.O.; Arum, C. Influence of some selected supplementary cementitious materials on workability and compressive strength of concrete—A review. *IOP Conf. Ser. Mater. Sci. Eng.* **2019**, *640*, 012071. [CrossRef]
17. Akinwumi, I.I.; Aidomojie, O.I. Effect of corncob ash on the geotechnical properties of lateritic soil stabilised with Portland cement. *Int. J. Geomat. Geosci.* **2015**, *5*, 375–392.
18. Isaia, G.C. High-performance concrete for sustainable constructions. *Waste Mater. Constr.* **2000**, *15*, 344–354.
19. Food and Agriculture Organization of the United Nations. *Food and Agriculture Organization Statistical Pocketbook World Food and Agriculture*; Food and Agriculture Organization of the United Nations: Rome, Italy, 2017.
20. Godjo, T.; Tagutchou, J.P.; Naquin, P.; Gourdon, R. Valorization des coques d'anacarde par pyrolyse au Benin. *Rev. Dechets Sci. Tech.* **2015**, *70*, 11–18.
21. BS EN 8615-2. Specification for Pozzolanic Materials for Use with Portland Cement. In *High Reactivity Natural Calcined Pozzo Lana*; BSI: London, UK, 2019.
22. BS EN 196-3. *Method of Testing Cement. Physical Test*; BSI: London, UK, 2016.
23. Khan, S.U.; Nuruddin, M.F.; Ayub, T.; Shafiq, N. Effects of different mineral admixtures on the properties of fresh concrete. *Sci. World J.* **2014**, *2004*, 986567. [CrossRef]
24. BS EN 12620. *Aggregates from Natural Sources for Concrete*; BSI: London, UK, 2013.
25. BS EN 206. *Concrete Specifications, Performance, Production and Conformity*; BSI: London, UK, 2016.
26. Pandi, K.; Anandakumar, R.; Ganesan, K. Study on optimum utilisation of groundnut shell ash and cashew nut shell ash in concrete. *Caribb. J. Sci.* **2018**, *53*, 981–991.
27. Oyebisi, S.; Igba, T.; Oniyide, D. Performance evaluation of cashew nutshell ash as a binder in concrete production. *Case Stud. Constr. Mater.* **2019**, *11*, e00293. [CrossRef]
28. BS EN 12350-2. *Testing Fresh Concrete. Method for Determination of Slump*; BSI: London, UK, 2019.

29. BS EN 12390-7. *Testing Hardened Concrete. Density of Hardened Concrete*; BSI: London, UK, 2019.
30. BS EN 12390-3. *Testing Hardened Concrete. Compressive Strength of Test Specimens*; BSI: London, UK, 2009.
31. Yu, Q.; Sawayama, K.; Sugita, S.; Shoya, M.; Isojima, Y. Reaction between rice husk ash and $Ca(OH)_2$ solution and the nature of its product. *Cem. Concr. Res.* **1999**, *29*, 37–43. [CrossRef]
32. Neville, A.M. *Properties of Concrete*, 5th ed.; Pearson Education Limited: London, UK, 2011.
33. Saygılı, A.; Baykal, G. A new method for improving the thermal insulation properties of fly ash. *Energy Build.* **2011**, *43*, 3236–3242. [CrossRef]
34. BS EN 1992-1-1. *Design of Concrete Structures. General Rules for Structural Fire Design*; BSI: London, UK, 2014.
35. Kaplan, M.F. Flexural and compressive strength of concrete as affected by the properties of coarse aggregates. *J. Am. Concr. Inst.* **1959**, *55*, 1193–1208.
36. Kumar, V.V.; Prasad, D.R. Influence of supplementary cementitious materials on strength and durability characteristics of concrete. *Adv. Concr. Constr.* **2019**, *7*, 75–85.
37. Duana, P.; Shuia, Z.; Chena, W.; Shenb, C. Enhancing microstructure and durability of concrete from ground granulated blast furnace slag and metakaolin as cement replacement materials. *J. Mater. Res. Technol.* **2013**, *2*, 52–59. [CrossRef]